Design of Linear-Phase Nonuniform Filter Banks With Partial Cosine Modulation

Wei Zhong, Guangming Shi, Xuemei Xie, and Xuyang Chen

***Abstract*—The majority of the existing work on designing nonuniform filter banks (NUFBs) cannot achieve linear-phase (LP) property, because of the high complexity associated with phase distribution. This correspondence proposes an idea of partial cosine modulation to obtain the LP property of NUFBs with rational sampling factors. It makes the efficient modulation technique possible to be used to design LP NUFBs. Except the separately designed lowpass and highpass analysis/synthesis filters, we obtain the bandpass by cosine modulation of several prototypes, worth of the name "partial cosine modulation." By analyzing the phase issue of significant aliasing terms, we derive the matching conditions to make the required LP NUFB achievable. With these criteria being satisfied, the design problem becomes that of several prototypes as well as the lowpass and highpass filters, leading to a less design effort. By using the proposed method, near-perfect-reconstruction LP NUFBs can be obtained in a simple and efficient way as demonstrated by examples.**

***Index Terms*—Linear-phase, nonuniform filter bank, near-perfect-reconstruction, partial cosine modulation.**

I. Introduction

Nonuniform filter banks(NUFBs) have been widely used in many signal processing applications due to their flexibility in partitioning subbands. In some cases, such as image coding, it is crucial for all filters to have linear-phase (LP) property. This is because LP filters can avoid artifacts in the reconstructed images.

It should be noticed that, among various methods of designing NUFBs [1]–[18], only a few are capable of achieving LP objective. In the indirect structure, the LP requirement was achieved in [9], where certain subbands of an LP uniform bank are recombined by synthesis filters of transmultiplexers. The NUFB so obtained has a long system delay due to the two-stage architecture. In contrast, the direct structure [10]–[18], which has only one stage, is more popular. In [10]–[14], the modulated NUFBs are constructed from uniform banks through transition filters or linear combination. However, due to the high complexity of phase distribution, there are no results about these designs on LP NUFBs. As to the direct design of individual nonuniform filters, some works have been done in [15]–[18]. Reference [15] presented a NUFB design based on the modulation of several prototypes. Unfortunately, the LP property of the resulting filters cannot be achieved either. Although the design in [16] adopts modulation technique to obtain the LP NUFB, the decimation filters with complex coefficients are required for the rational case to reduce the aliasing distortion. Reference [17] formulates the perfect-reconstruction (PR) constraints in a quadratic form of filter coefficients so as to avoid the nonlinear optimization. But as for the LP NUFBs, it only considers the necessary conditions on integer sampling factors implemented by a binary tree. In our previous work [18], a direct design was proposed for LP near-PR (NPR) NUFBs with rational sampling factors. But the individual implementation of all M filters leads to an extremely computational load compared to the modulated bank which only needs the design of several prototypes. Thus, in this context, it is valuable to exploit the efficient design of NUFBs with LP property.

Manuscript received October 11, 2009; accepted February 09, 2010. Date of publication March 11, 2010; date of current version May 14, 2010. The associate editor coordinating the review of this manuscript and approving it for publication was Prof. Jean-Christophe Pesquet. This work was supported by the Program for New Century Excellent Talents (No. NCET-07-0656), the NSFC (Nos. 60736043, 60776795), and by the Ph.D. Program Foundation of Ministry of Education of China (Nos. 200807010004, 20090203110003). The material in this paper was presented in part at the IEEE International Conference Communications, Circuits, and Systems, Guilin, China, June 2006.

The authors are with the School of Electronic Engineering, Xidian University, Xi'an 710071, China (e-mail: wzhong@mail.xidian.edu.cn; gmshi@mail.xidian.edu.cn; xmxie@mail.xidian.edu.cn, xychen@mail.xidian.edu.cn).

Digital Object Identifier 10.1109/TSP.2010.2045424

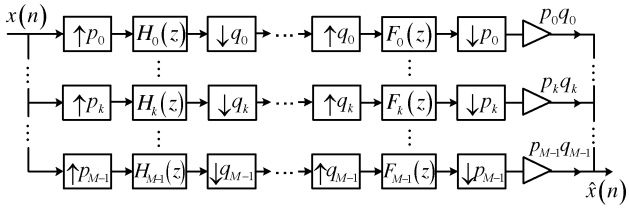

Fig. 1. Direct structure of M-channel NUFB with rational sampling factors.

In this correspondence, a method called partial cosine modulation is proposed for designing LP NUFBs with rational sampling factors. It takes advantage of modulation technique while maintaining the LP property of individual filters. In the proposed method, we design the lowpass and highpass analysis/synthesis filters separately, and obtain the bandpass by cosine modulation of several prototypes, worth of the name "partial cosine modulation". With a rigorous analysis of phase issue, the matching conditions are derived to obtain the required LP NUFB. By using the proposed method, the requirements for the entire LP NUFB design are simply represented as those imposed on several prototypes as well as the lowpass and highpass filters, leading to a less design effort. In addition, the proposed LP NUFB is based on the one-stage direct structure and thus has lower system delay. As illustrated by examples, the proposed method can provide a simple and efficient alternative for designing NPR NUFBs with the expected LP property.

The rest of this correspondence is organized as follows. Section II describes the idea of partial cosine modulation. Section III analyzes the significant aliasing cancellation, followed by the filter design and examples in Section IV and conclusions in Section V.

II. Idea of Partial Cosine Modulation

Fig. 1 shows the direct structure of M-channel NUFB with rational sampling factors $p_k/q_k, 0 \le k \le M-1$. In the modulated NUFB, each pair of the analysis and synthesis filters, $h_k(n)$ and $f_k(n)$, are obtained by the cosine modulation of an LP prototype filter $p_k(n)$,

$$\begin{aligned} h_k(n) &= 2p_k(n)\cos\left((2m_k+1)\frac{\pi}{2q_k}\left(n-\frac{N_k}{2}\right)+\theta_k\right), \\ f_k(n) &= 2p_k(n)\cos\left((2m_k+1)\frac{\pi}{2q_k}\left(n-\frac{N_k}{2}\right)-\theta_k\right) \\ &= h_k(N_k-n) \end{aligned} \tag{1}$$

where $0 \le k \le M-1, 0 \le n \le N_k$. N_k is the order of $p_k(n)$, m_k is the position parameter which selects the frequency interval extracted by $h_k(n)$ and $f_k(n)$, and θ_k is the modulation phase.

In the modulated NUFB proposed in [15], θ_k is chosen as $\{\pi/4 \text{ or } -\pi/4\}$ subjected to the conditions for canceling different types of aliasing couplings in adjacent channels. The detailed explanation of those types of aliasing couplings will be given in Section III-A. Thus the resulting filters do not possess LP property. Our target is to achieve the LP property of individual filters relying on the efficient modulation technique. This additional phase requirement for the LP objective makes the design problem quite different.

Next we derive the proposed method of partial cosine modulation. We first consider how to obtain the LP property of $h_k(n)$ and $f_k(n)$ modulated from (1). For the convenience of analysis, we write their frequency responses as the sum of positive and negative frequency components, denoted by $U_k(e^{j\omega})$ and $V_k(e^{j\omega})$:

$$\begin{aligned} H_k(e^{j\omega}) &= e^{j\theta_k}U_k(e^{j\omega}) + e^{-j\theta_k}V_k(e^{j\omega}) \\ F_k(e^{j\omega}) &= e^{-j\theta_k}U_k(e^{j\omega}) + e^{j\theta_k}V_k(e^{j\omega}) \end{aligned} \tag{2}$$

and

$$\begin{aligned} U_k(e^{j\omega}) &= e^{-j\omega N_k/2}P_{kR}(\omega - \pi(2m_k+1)/2q_k) \\ V_k(e^{j\omega}) &= e^{-j\omega N_k/2}P_{kR}(\omega + \pi(2m_k+1)/2q_k) \end{aligned} \tag{3}$$

where $P_{kR}(\omega)$ is the amplitude response of the prototype $P_k(e^{j\omega})$. Substituting (3) into (2), we can see that to ensure the LP property of $H_k(e^{j\omega})$ and $F_k(e^{j\omega})$, $e^{j\theta_k}$ should be chosen as $\{1 \text{ or } -1\}$ for symmetry and $\{j \text{ or } -j\}$ for antisymmetry. Correspondingly, θ_k has to be selected as $\{0 \text{ or } \pi\}$ and $\{\pi/2 \text{ or } -\pi/2\}$.

With regard to amplitude distortion, we turn our attention to the overall transfer function $T(z)$ of the system shown in Fig. 1

$$T(z) = \sum_{k=0}^{M-1}\sum_{i_k=0}^{p_k-1} H_k\left(z^{1/p_k}W_{p_k}^{i_k}\right)F_k\left(z^{1/p_k}W_{p_k}^{i_k}\right) \tag{4}$$

where $W_{p_k}^{i_k} = e^{-j2\pi i_k/p_k}$. Substituting (2) into (4) with $z = e^{j\omega}$, we get

$$\begin{aligned} T(e^{j\omega}) = &\sum_{k=0}^{M-1}\sum_{i_k=0}^{p_k-1}\left(U_k^2\left(e^{j\omega/p_k}W_{p_k}^{i_k}\right) + V_k^2\left(e^{j\omega/p_k}W_{p_k}^{i_k}\right)\right) \\ &+ \sum_{k=0}^{M-1}(e^{j2\theta_k} + e^{-j2\theta_k}) \\ &\times \sum_{i_k=0}^{p_k-1} U_k\left(e^{j\omega/p_k}W_{p_k}^{i_k}\right)V_k\left(e^{j\omega/p_k}W_{p_k}^{i_k}\right). \end{aligned} \tag{5}$$

Since $\sum_{i_k=0}^{p_k-1} U_k(e^{j\omega/p_k}W_{p_k}^{i_k})$ and $\sum_{i_k=0}^{p_k-1} V_k(e^{j\omega/p_k}W_{p_k}^{i_k})$ do not overlap significantly except when $k = 0$ and $M-1$, (5) can be simplified into

$$\begin{aligned} &T(e^{j\omega}) \\ &\approx \left(e^{j2\theta_0} + e^{-j2\theta_0}\right)\sum_{i_0=0}^{p_0-1} U_0\left(e^{j\omega/p_0}W_{p_0}^{i_0}\right)V_0\left(e^{j\omega/p_0}W_{p_0}^{i_0}\right) \\ &\quad + (e^{j2\theta_{M-1}} + e^{-j2\theta_{M-1}})\sum_{i_{M-1}=0}^{p_{M-1}-1} U_{M-1}\left(e^{j\omega/p_{M-1}}W_{p_{M-1}}^{i_{M-1}}\right) \\ &\quad \times V_{M-1}\left(e^{j\omega/p_{M-1}}W_{p_{M-1}}^{i_{M-1}}\right) \\ &\quad + \sum_{k=0}^{M-1}\sum_{i_k=0}^{p_k-1}\left(U_k^2\left(e^{j\omega/p_k}W_{p_k}^{i_k}\right) + V_k^2\left(e^{j\omega/p_k}W_{p_k}^{i_k}\right)\right). \end{aligned} \tag{6}$$

Under the analysis of (2) on the LP requirement of selecting θ_0 and θ_{M-1} being $\{0 \text{ or } \pi\}$ for symmetry and θ_{M-1} being $\{\pi/2 \text{ or } -\pi/2\}$ for antisymmetry, the first two cross-terms in (6), $\sum_{i_0=0}^{p_0-1} U_0(e^{j\omega/p_0}W_{p_0}^{i_0})V_0(e^{j\omega/p_0}W_{p_0}^{i_0})$ and $\sum_{i_{M-1}=0}^{p_{M-1}-1} U_{M-1}(e^{j\omega/p_{M-1}}W_{p_{M-1}}^{i_{M-1}})V_{M-1}(e^{j\omega/p_{M-1}}W_{p_{M-1}}^{i_{M-1}})$, can create significant distortions around the frequencies $\omega = 0$ and $\omega = \pi$ in $-\pi \le \omega < \pi$.

Therefore, in order to cancel these amplitude distortions while maintaining the LP property of individual filters, we have to design the lowpass filter $h_0(n)$ and highpass filter $h_{M-1}(n)$ separately, whereas obtaining the bandpass $h_k(n), 1 \le k \le M-2$, by cosine modulation of $p_k(n)$ with θ_k selected being $\{0 \text{ or } \pi\}$ for symmetry and $\{\pi/2 \text{ or } -\pi/2\}$ for antisymmetry. That is why this method is called partial cosine modulation. In our work, the same prototype is used in channels with the same sampling factors. The analysis and synthesis filters hold the time-reverse relation, i.e., $f_k(n) = h_k(N_k - n)$.

Unlike the conventional non-LP modulated NUFB [15], the additional LP requirement makes the proposed method sacrifice the identity of designing all filters by modulation. Thus, the issue on the matching of individual LP filters needs to be considered. In what follows, we will analyze the significant aliasing cancellation, deriving the matching conditions of all the LP filters involved that make the proposed LP NUFB achievable.

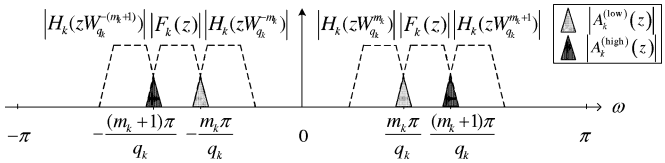

Fig. 2. Overlapped components of $H_k(zW_{q_k}^{l_k})F_k(z)$.

III. Cancellation of Significant Aliasing Distortion

A. Four Types of Aliasing Couplings

From the direct structure of NUFBs shown in Fig. 1, we can obtain the expression of aliasing term $A_{k,l_k}(z)$ as

$$A_{k,l_k}(z) = \sum_{i_k=0}^{p_k-1} H_k\left(z^{1/p_k}W_{p_k}^{i_k}W_{q_k}^{l_k}\right)F_k\left(z^{1/p_k}W_{p_k}^{i_k}\right) \tag{7}$$

where $0 \le k \le M-1, 1 \le l_k \le q_k - 1$, and $W_{q_k}^{l_k} = e^{-j2\pi l_k/q_k}$. Clearly, it can be regarded as the decimated version of $H_k(zW_{q_k}^{l_k})F_k(z)$ by p_k

$$A_{k,l_k}(z) = p_k H_k\left(zW_{q_k}^{l_k}\right)F_k(z) \downarrow p_k. \tag{8}$$

We analyze $H_k(zW_{q_k}^{l_k})F_k(z)$ first. Under the assumption that the stopband attenuation is high enough, $H_k(zW_{q_k}^{l_k})$ and $F_k(z)$ do not overlap significantly except when $l_k = \pm m_k$ and $l_k = \pm(m_k+1)$. Fig. 2 illustrates those overlapped components which are combined into two pairs. One pair $A_k^{(\text{low})}(z)$ is $\{H_k(zW_{q_k}^{m_k})F_k(z), H_k(zW_{q_k}^{-m_k})F_k(z)\}$, located at $\pm m_k\pi/q_k$ as its central frequencies in $-\pi \le \omega < \pi$. The other pair $A_k^{(\text{high})}(z)$ is $\{H_k(zW_{q_k}^{m_k+1})F_k(z), H_k(zW_{q_k}^{-(m_k+1)})F_k(z)\}$ at $\pm(m_k+1)\pi/q_k$. The notations $A_k^{(\text{low})}(z)$ and $A_k^{(\text{high})}(z)$ denote the overlaps produced at the low-frequency and high-frequency transition bands of $F_k(z)$, respectively.

Back to (8), we analyze $A_{k,l_k}(z)$ with $H_k(zW_{q_k}^{l_k})F_k(z)$ replaced by $A_k^{(\text{low})}(z)$ and $A_k^{(\text{high})}(z)$. After downsampling by p_k, the resulting significant aliasing $p_k A_k^{(\text{low})}(z) \downarrow p_k$ may locate at $\pm\sum_{i=0}^{k-1} p_i\pi/q_i$ or $\pm\sum_{i=0}^{k} p_i\pi/q_i$ as its central frequencies in $-\pi \le \omega < \pi$, and $p_k A_k^{(\text{high})}(z) \downarrow p_k$ at $\pm\sum_{i=0}^{k} p_i\pi/q_i$ or $\pm\sum_{i=0}^{k-1} p_i\pi/q_i$. For easy comprehension, Fig. 3 illustrates in the top the case that $p_k A_k^{(\text{low})}(z) \downarrow p_k$ locates around $\pm\sum_{i=0}^{k-1} p_i\pi/q_i$ and $p_k A_k^{(\text{high})}(z) \downarrow p_k$ around $\pm\sum_{i=0}^{k} p_i\pi/q_i$ as an example. The similar analysis procedures can also be applied to the adjacent channels, say $(k-1)$th or $(k+1)$th. Fig. 3 also shows in the bottom the case in the $(k+1)$th channel with $p_{k+1}A_{k+1}^{(\text{low})}(z) \downarrow p_{k+1}$ locating around $\pm\sum_{i=0}^{k+1} p_i\pi/q_i$ and $p_{k+1}A_{k+1}^{(\text{high})}(z) \downarrow p_{k+1}$ around $\pm\sum_{i=0}^{k} p_i\pi/q_i$.

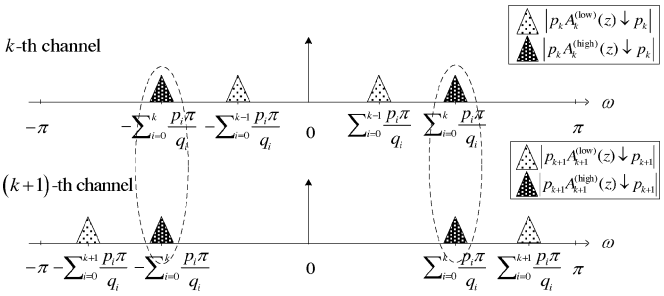

Fig. 3. Significant aliasing terms in the kth and $(k+1)$th channels.

It can be seen clearly, one aliasing term in the kth channel can be coupled with the one in the $(k+1)$th channel having same central frequencies $\pm\sum_{i=0}^{k} p_i\pi/q_i$ as circled in Fig. 3, forming an aliasing *coupling*. As to the other aliasing term in the kth channel, it can be coupled with the one in the $(k-1)$th channel locating around the same position $\pm\sum_{i=0}^{k-1} p_i\pi/q_i$. Those *couplings* have four types in adjacent channels, leading to significant aliasing cancellation [15]:

$$\text{high}-\text{high type}, p_k A_k^{(\text{high})}(z)\downarrow p_k + p_{k+1}A_{k+1}^{(\text{high})}(z)\downarrow p_{k+1}=0 \tag{9a}$$

$$\text{high}-\text{low type}, p_k A_k^{(\text{high})}(z)\downarrow p_k + p_{k+1}A_{k+1}^{(\text{low})}(z)\downarrow p_{k+1}=0 \tag{9b}$$

$$\text{low}-\text{high type}, p_k A_k^{(\text{low})}(z)\downarrow p_k + p_{k+1}A_{k+1}^{(\text{high})}(z)\downarrow p_{k+1}=0 \tag{9c}$$

$$\text{low}-\text{low type}, p_k A_k^{(\text{low})}(z)\downarrow p_k + p_{k+1}A_{k+1}^{(\text{low})}(z)\downarrow p_{k+1}=0 \tag{9d}$$

where $0\le k\le M-2$. Further, we notice that in each coupling, if the magnitude responses of the two aliasing terms have the same amount at the same frequency point and their phases are chosen to differ by π, the significant aliasing can be cancelled completely.

B. Phase Property of Aliasing Couplings in Adjacent Channels

In the proposed partial modulated bank, $H_k(z), 1\le k\le M-2$, are modulated from the prototypes $P_k(z)$, whereas $H_0(z)$ and $H_{M-1}(z)$ are designed separately. For the convenience of discussion, we classify those couplings in adjacent channels into two cases: 1) bandpass and 2) lowpass and highpass.

1) Bandpass: For the cancellation of aliasing couplings in adjacent channels from the 1th to $(M-2)$th, corresponding to the bandpass $H_k(z)$ modulated from (1), $1\le k\le M-2$, the conditions on the modulation phase θ_k have been given in [15]. Different from [15], in our work to obtain the LP property, we select θ_k to be $\{\pi/2 \text{ or } -\pi/2\}$ and $\{0 \text{ or } \pi\}$ alternately. Moreover, for whole system, since the lowpass $H_0(z)$ must be symmetric, we have to select θ_1 in the modulation of the first bandpass $H_1(z)$ to begin with $\{\pi/2 \text{ or } -\pi/2\}$. The matching condition between the separately designed $H_0(z)$ and modulated $H_1(z)$ will be analyzed in the next case.

2) Lowpass and Highpass: This case corresponds to the aliasing cancellation in the lowpass filter and the first bandpass filter, as well as that in the last bandpass filter and the highpass filter.

For the lowpass filter, since $H_0(zW_{q_0}^{l_0})F_0(z)$ involves only one pair $A_0^{(\text{high})}(z)$ with $l_0=\pm(m_0+1)=\pm 1$, only two types of couplings in (9) should be considered in the 0th and 1th channels. They are *high-high* type in (9a) and *high-low* type in (9b) with $k=0$. Similarly for the aliasing cancellation in the $(M-2)$th and $(M-1)$th channels, only two types of couplings should be focused on, *high-low* type in (9b) and *low-low* type in (9d) with $k=M-2$.

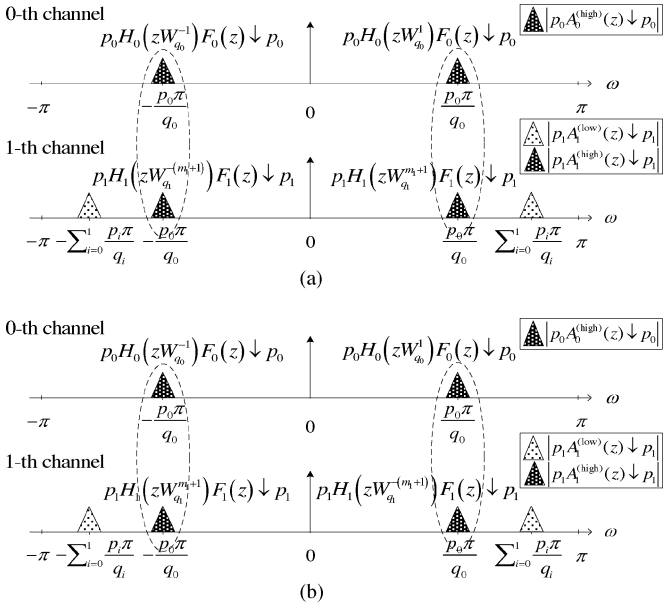

Fig. 4. Aliasing terms $p_0A_0^{(\text{high})}(z)\downarrow p_0$ and $p_1A_1^{(\text{high})}(z)\downarrow p_1$ with the case that (a) $p_1H_1(zW_{q_1}^{m_1+1})F_1(z)\downarrow p_1$ locates around $p_0\pi/q_0$. (b) $p_1H_1(zW_{q_1}^{-(m_1+1)})F_1(z)\downarrow p_1$ locates around $p_0\pi/q_0$.

Since similar analysis procedures can be applied to above four types, we analyze the phase property of *high-high* type in the 0th and 1th channels as an example. With $k=0$, (9a) becomes

$$p_0A_0^{(\text{high})}(z)\downarrow p_0 + p_1A_1^{(\text{high})}(z)\downarrow p_1 = 0. \tag{10}$$

For the first term, $A_0^{(\text{high})}(z)$ after downsampled by p_0 becomes the pair $\{p_0H_0(zW_{q_0}^{1})F_0(z)\downarrow p_0, p_0H_0(zW_{q_0}^{-1})F_0(z)\downarrow p_0\}$. They locate, respectively, at $p_0\pi/q_0$ and $-p_0\pi/q_0$ as their central frequencies in $[-\pi,\pi)$, shown in the top of Fig. 4(a). For the second term, $A_1^{(\text{high})}(z)$ after downsampled by p_1 becomes $\{p_1H_1(zW_{q_1}^{m_1+1})F_1(z)\downarrow p_1, p_1H_1(zW_{q_1}^{-(m_1+1)})F_1(z)\downarrow p_1\}$. Their locations may produce two cases. One is that $p_1H_1(zW_{q_1}^{m_1+1})F_1(z)\downarrow p_1$ locates at $p_0\pi/q_0$ as its central frequency in $[-\pi,\pi)$ and $p_1H_1(zW_{q_1}^{-(m_1+1)})F_1(z)\downarrow p_1$ at $-p_0\pi/q_0$, illustrated in the bottom of Fig. 4(a). The other is that $p_1H_1(zW_{q_1}^{-(m_1+1)})F_1(z)\downarrow p_1$ locates around $p_0\pi/q_0$ and $p_1H_1(zW_{q_1}^{m_1+1})F_1(z)\downarrow p_1$ around $-p_0\pi/q_0$, illustrated in the bottom of Fig. 4(b). For clear description, the pair $\{p_0H_0(zW_{q_0}^{1})F_0(z)\downarrow p_0, p_0H_0(zW_{q_0}^{-1})F_0(z)\downarrow p_0\}$ in the 0th channel is illustrated again in the top of Fig. 4(b). Since both cases lead to the same result, we take the case illustrated in Fig. 4(a) as an example.

For two aliasing terms within the coupling illustrated in Fig. 4(a), $p_0A_0^{(\text{high})}(z)\downarrow p_0$ and $p_1A_1^{(\text{high})}(z)\downarrow p_1$, we can get their positive frequency components locating around $p_0\pi/q_0$ in $[-\pi,\pi)$ as

$$\begin{aligned} &p_0H_0\left(zW_{q_0}^{1}\right)F_0(z)\downarrow p_0 \\ &\quad\overset{z=e^{j\omega}}{\rightarrow} p_0H_0(e^{j(\omega-2\pi/q_0)})F_0(e^{j\omega})\downarrow p_0 \\ &\quad= e^{-j\omega N_0/p_0}e^{j\pi N_0/q_0} \\ &\qquad\times H_{0R}(\omega/p_0-2\pi/q_0)H_{0R}(\omega/p_0) \end{aligned} \tag{11}$$

$$\begin{aligned} &p_1H_1\left(zW_{q_1}^{m_1+1}\right)F_1(z)\downarrow p_1 \\ &\quad\overset{z=e^{j\omega}}{\rightarrow} p_1H_1(e^{j(\omega-2\pi(m_1+1)/q_1)})F_1(e^{j\omega})\downarrow p_1 \\ &\quad= e^{-j2\theta_1}e^{-j\omega N_1/p_1}e^{j\pi N_0/q_0} \\ &\qquad\times P_{1R}(\omega/p_1-p_0\pi/q_0p_1-\pi/2q_1) \\ &\qquad\cdot P_{1R}(\omega/p_1-p_0\pi/q_0p_1+\pi/2q_1) \end{aligned} \tag{12}$$

where $H_{0R}(\omega)$ is the amplitude response of lowpass filter $H_0(e^{j\omega})$, and $P_{1R}(\omega)$ is that of the prototype $P_1(e^{j\omega})$ in the 1th channel. The detailed derivations of (11) and (12) are given in Appendix.

From (11) and (12), it can be seen that the phases of the two components are $-\omega N_0/p_0 + \pi N_0/q_0$ and $-\omega N_1/p_1 + \pi N_0/q_0 - 2\theta_1$. Without considering the sign term $-2\theta_1$, to make the two phases being same, the analysis filters need to satisfy the following condition on the orders N_k and sampling factors $p_k, 0 \le k \le M-1$

$$N_0/p_0 = N_1/p_1 = \cdots = N_k/p_k = \cdots = N_{M-1}/p_{M-1}. \quad (13)$$

Considering the sign term $-2\theta_1$ in (12), we have to select θ_1 to be $\{\pi/2 \text{ or } -\pi/2\}$ to make the above two phases differ by π. Recalling the analysis of (2) that θ_k should be chosen as $\{0 \text{ or } \pi\}$ for symmetry and $\{\pi/2 \text{ or } -\pi/2\}$ for antisymmetry, we conclude $H_1(z)$ must be antisymmetric. Similarly for negative frequency components of two aliasing terms within the coupling illustrated in Fig. 4(a), we can get the same result.

C. Conditions for Significant Aliasing Cancellation

In the proposed partial modulated LP NUFB, we assume that $h_k(n)$ and $f_k(n)$ hold the time-reverse relation and the filter orders fulfill (13). Then the findings up to now can be summarized for the cancellation of significant aliasing distortion:

a) The analysis filters $h_k(n), 0 \le k \le M-1$, satisfy an alternate symmetry property, that is, $h_k(n)$ are symmetric and antisymmetric alternately.

b) The magnitude responses of the two aliasing terms within each coupling need to have the same amount at the same frequency point. That is, the stretched transition bands of $p_k(n), 1 \le k \le M-2, h_0(n)$ and $h_{M-1}(n)$ after downsampled by the corresponding p_k should have the same shape.

IV. Filter Design and Examples

Under the assumption that the stopband attenuation is sufficiently high and the passband is flat enough, to achieve the NPR property, we need consider only the amplitude distortion at the transition bands of adjacent filters. In the proposed partial modulated bank, the following constraints should be satisfied among the lowpass filter $H_0(e^{j\omega})$, prototypes $P_k(e^{j\omega}), 1 \le k \le M-2$, and highpass filter $H_{M-1}(e^{j\omega})$:

$$|H_0(e^{j\omega/p_0})|^2 + |P_1(e^{j(\omega-\varphi_1)/p_1})|^2 = 1 \quad (14)$$
$$p_0(\pi/q_0 - \varepsilon_0) < \omega < p_0(\pi/q_0 + \varepsilon_0)$$
$$\varphi_1 = p_0\pi/q_0 + p_1\pi/2q_1$$
$$|P_k(e^{j\omega/p_k})|^2 + |P_{k+1}(e^{j(\omega-\varphi_{k+1})/p_{k+1}})|^2 = 1 \quad 1 \le k \le M-3, \quad (15)$$
$$p_k(\pi/2q_k - \varepsilon_k) < \omega < p_k(\pi/2q_k + \varepsilon_k),$$
$$\varphi_{k+1} = p_k\pi/2q_k + p_{k+1}\pi/2q_{k+1}$$
$$|P_{M-2}(e^{j(\omega-\varphi_{M-1})/p_{M-2}})|^2 + |H_{M-1}(e^{j\omega/p_{M-1}})|^2 = 1$$
$$p_{M-1}\left(\frac{(q_{M-1}-1)\pi}{q_{M-1}} - \varepsilon_{M-1}\right) < \omega < p_{M-1}\left(\frac{(q_{M-1}-1)\pi}{q_{M-1}} + \varepsilon_{M-1}\right),$$
$$\varphi_{M-1} = p_{M-1}(q_{M-1}-1)\pi/q_{M-1} - p_{M-2}\pi/2q_{M-2} \quad (16)$$

where ε_k takes the half of the transition bandwidth, $0 \le k \le M-1$. The above requirements would be met by forcing the stretched transition bands of adjacent filters to follow the cosine roll-off characteristics. Interested readers please refer to [9]. By doing so, the second condition in Section III-C can also be satisfied.

The proposed LP NUFB can be performed by using one of the available filter design tools. In this paper, we employ the Parks-McClellan algorithm for illustration. The Parks-McClellan algorithm for filter design has the optimal solution in the minimax sense with respect to the specified magnitude response of the filter and it can easily be used by the function *FIRPM* in MATLAB. By those good properties, we use this algorithm to specify the transition bands of adjacent filters so as to make their stretched versions approximate the cosine roll-off characteristics, thereby simplifying the design of the desired LP NUFB.

The systematic design procedures of the proposed LP NUFB are summarized below. The filters involved are all designed by the Parks-McClellan algorithm with the stretched transition bands having the form of cosine roll-off function. Given the rational sampling factors $[p_k/q_k], 0 \le k \le M-1$, with $\sum_{k=0}^{M-1} p_k/q_k = 1$

1) Choose the filter orders $N_0/p_0 = \cdots = N_k/p_k = \cdots = N_{M-1}/p_{M-1}$, satisfying (13).
2) Design the symmetric lowpass filter $H_0(e^{j\omega})$ with order N_0, cutoff frequency $\omega_{0\_c} = \pi/q_0$ and transition bandwidth $2\varepsilon_0$.
3) Design the prototypes $P_k(e^{j\omega}), 1 \le k \le M-2$, with order N_k, cutoff frequency $\omega_{P_k\_c} = \pi/2q_k$ and transition bandwidth $2\varepsilon_k$.
4) Obtain the modulated bandpass filters $H_k(e^{j\omega}), 1 \le k \le M-2$, using (1), with θ_k selected to be $\{\pi/2 \text{ or } -\pi/2\}$ and $\{0 \text{ or } \pi\}$ alternately, and m_k chosen to extract the feasible frequency component of input signal upsampled by p_k.
5) Design the highpass filter $H_{M-1}(e^{j\omega})$ with order N_{M-1}, cutoff frequency $\omega_{M-1\_c} = (q_{M-1}-1)\pi/q_{M-1}$ and transition bandwidth $2\varepsilon_{M-1}$. $H_{M-1}(e^{j\omega})$ is symmetric for odd M, and is antisymmetric for even M.
6) Set $p_0\varepsilon_0 = \cdots = p_k\varepsilon_k = \cdots = p_{M-1}\varepsilon_{M-1}$ to make sure that the stretched transition bands of $H_0(e^{j\omega}), P_k(e^{j\omega}), 1 \le k \le M-2$, and $H_{M-1}(e^{j\omega})$ after downsampled by the corresponding p_k have the same bandwidth.

Now we give two examples to illustrate the performance of the proposed method.

Example 1: In this example, a 2-channel LP NUFB is considered as a comparison to the recombination one shown in the first example of [9]. They have the same sampling factors [3/4, 1/4]. Under the similar design specifications, such as transition bandwidth and stopband attenuation, we choose the filter orders to be $N_0 = 177, N_1 = 59$. Following the design procedures given above, we design the symmetric lowpass filter $H_0(e^{j\omega})$ and antisymmetric highpass filter $H_1(e^{j\omega})$ to achieve the required LP NUFB. Fig. 5 shows respectively the magnitude responses of the analysis filters, as well as aliasing and amplitude distortions. The maximum value of aliasing error E_a and peak-to-peak value of amplitude distortion E_{pp} are $E_a = 3.005 \times 10^{-3}, E_{\text{pp}} = 7.822 \times 10^{-3}$. The stopband attenuation is about 67.4 dB. This performance is comparable to that of [9] which has a PR violation of 10^{-3} and stopband attenuation around 65 dB.

Further we compare the proposed method with indirect structure [9] in terms of system delay and implementation complexity as summarized in Table I. The implementation complexity is measured by the number of the required multiplications per unit-time (MPU) and additions per unit-time (APU). From Table I we can see that, our proposed LP NUFB is a low-delay system. Compared with indirect structure [9], the system delay of the proposed method is almost only one-third of that of [9] (59 versus 167), at the expense of higher complexity. Such a low-delay system is very crucial for those delay sensitive applications.

Example 2: This example is a 4-channel LP NUFB with sampling factors [2/7, 2/7, 2/7, 1/7]. The filter orders are $N_0 = N_1 = N_2 = 162, N_3 = 81$. In this example $p_1/q_1 = p_2/q_2$, we need design only one prototype for modulating two bandpass filters. In the modulation formula (1), we select the position parameters $m_1 = 5, m_2 = 4$. And the modulation phases are $\theta_1 = \pi/2, \theta_2 = 0$. By the above design procedures, we obtain the desired result shown in Fig. 6. The aliasing and amplitude distortions are $E_a = 1.484 \times 10^{-4}, E_{\text{pp}} = 2.783 \times 10^{-3}$, respectively. And the stopband attenuation is 87.8 dB.

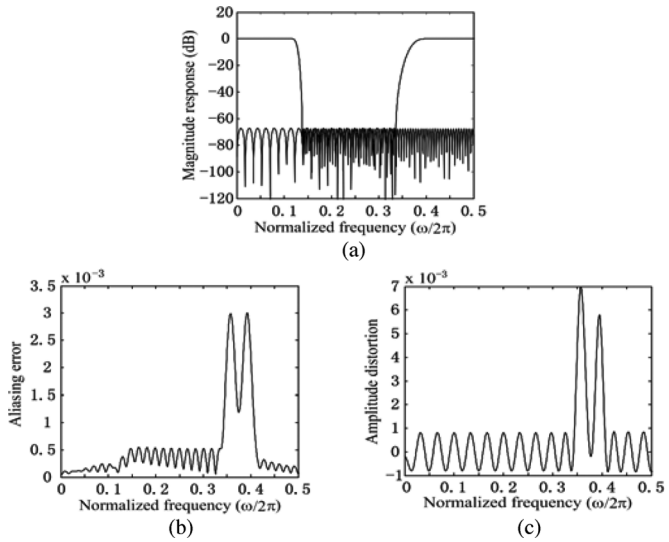

Fig. 5. The 2-channel LP NUFB with sampling factors [3/4, 1/4]. (a) Magnitude responses of analysis filters. (b) Aliasing error. (c) Amplitude distortion.

TABLE I
COMPARISON BETWEEN THE PROPOSED METHOD AND EXISTING TYPICAL LP NUFB DESIGNS [9], [18]

Example 1: $[3/4, 1/4]$	Indirect Structure [9]	Proposed Method
Filter Order	$N_M = 83,\ N_{m_0} = 62$	$N_0 = 177,\ N_1 = 59$
System Delay	167	59
MPU	133 $\{*482\}$	149 $\{*594\}$
APU	131 $\{*476\}$	148 $\{*590\}$
Example 2: $[2/7, 2/7, 2/7, 1/7]$	**Direct Design of Individual LP Filters [18]**	**Proposed Method**
Filter Order	$N_0 = N_1 = N_2 = 162,$ $N_3 = 81$	$N_0 = N_1 = N_2 = 162,$ $N_3 = 81$
System Delay	81	81
MPU	151 $\{*1060\}$	105 $\{*734\}$
APU	150 $\{*1053\}$	104 $\{*729\}$

$\{*-\}$ Direct implementation without using polyphase decomposition.

For this example, we compare the proposed method with direct design of individual LP filters [18]. Under the same design specifications, we simulate this example by the method given in [18], which is the authors' previous work. The simulation result shows that the two direct design methods can achieve comparable stopband attenuation, aliasing error, and amplitude distortion. But from the comparison shown in Table I, we can see that the design and implementation complexities of our method are much lower than that of [18]. This is because in our method, two LP bandpass filters are obtained by modulating one prototype, thanks to the efficient modulation technique. It should be noticed that in the proposed LP NUFB, the more the channels having the same sampling factors, the more the filters modulated from several prototypes, and, thus, the less the implementation complexity.

V. CONCLUSION

In this correspondence, particular attention has been paid to the problem of achieving the LP property of NUFBs relying on the modulation technique. As a solution, a method called partial cosine modulation is proposed. With the matching conditions of all LP filters involved satisfied, the design problem of LP NUFBs can be simplified into that of the prototype filters, leading to a less design effort. Two examples and comparison results show that under the similar design specifications, the proposed method has lower system delay than the indirect structure [9] and lower implementation complexity than the direct design of individual LP filters [18].

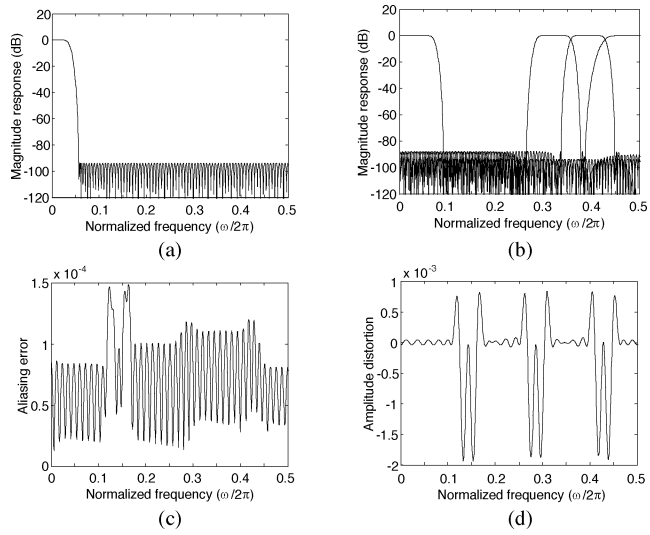

Fig. 6. The 4-channel LP NUFB with sampling factors [2/7, 2/7, 2/7, 1/7]. (a) Magnitude response of prototype filter. (b) Magnitude responses of analysis filters. (c) Aliasing error. (d) Amplitude distortion.

APPENDIX
DERIVATIONS OF (11) AND (12)

Consider the coupling of *high-high* type in the 0th and 1th channels shown in (10). It consists of two aliasing terms, $p_0 A_0^{(\mathrm{high})}(z) \downarrow p_0$ and $p_1 A_1^{(\mathrm{high})}(z) \downarrow p_1$. We analyze their positive frequency components in the case illustrated in Fig. 4(a).

For the first term $p_0 A_0^{(\mathrm{high})}(z) \downarrow p_0$, its positive frequency component is $p_0 H_0(zW_{q_0}^1) F_0(z) \downarrow p_0$. It locates at $p_0\pi/q_0$ as its central frequency in $[-\pi, \pi)$, shown in the top of Fig. 4(a). We analyze $H_0(zW_{q_0}^1)F_0(z)$ first. Since the LP lowpass filter $h_0(n)$ has to be symmetric, that is, $h_0(n) = h_0(N_0 - n)$. Under the time-reverse relation $f_k(n) = h_k(N_k - n)$ with $k = 0$, we obtain

$$f_0(n) = h_0(n) \text{ or } F_0(z) = H_0(z). \tag{17}$$

Substituting (17) and the expression of symmetric $H_0(e^{j\omega})$, i.e., $H_0(e^{j\omega}) = e^{-j\omega N_0/2} H_{0R}(\omega)$, $H_0(zW_{q_0}^1)F_0(z)$ becomes

$$\begin{aligned} H_0\left(zW_{q_0}^1\right) F_0(z) &\overset{z=e^{j\omega}}{\longrightarrow} H_0(e^{j(\omega-2\pi/q_0)}) F_0(e^{j\omega}) \\ &= e^{-j\omega N_0} e^{j\pi N_0/q_0} \\ &\quad \times H_{0R}(\omega - 2\pi/q_0) H_{0R}(\omega). \end{aligned} \tag{18}$$

After downsampled by p_0, (18) becomes

$$\begin{aligned} & p_0 H_0\left(zW_{q_0}^1\right) F_0(z) \downarrow p_0 \\ &\quad \overset{z=e^{j\omega}}{\longrightarrow} p_0 H_0(e^{j(\omega-2\pi/q_0)}) F_0(e^{j\omega}) \downarrow p_0 \\ &\quad = \sum_{i_0=0}^{p_0-1} e^{-j(\omega-2\pi i_0)N_0/p_0} e^{j\pi N_0/q_0} \\ &\qquad \times H_{0R}((\omega - 2\pi i_0)/p_0 - 2\pi/q_0) \\ &\qquad \times H_{0R}((\omega - 2\pi i_0)/p_0). \end{aligned} \tag{19}$$

With $i_0 = 0$, we get its response in $[-\pi, \pi)$ as expressed in (11).

For the second term $p_1 A_1^{(\text{high})}(z) \downarrow p_1$, its positive frequency component is $p_1 H_1(zW_{q_1}^{m_1+1})F_1(z) \downarrow p_1$. It locates around the same position as that of the first term, shown in the bottom of Fig. 4(a). We also consider $H_1(zW_{q_1}^{m_1+1})F_1(z)$ first. Substituting (2) and (3), $H_1(zW_{q_1}^{m_1+1})F_1(z)$ becomes

$$\begin{aligned} H_1\left(zW_{q_1}^{m_1+1}\right)F_1(z) &\overset{z=e^{j\omega}}{\longrightarrow} H_1(e^{j(\omega-2\pi(m_1+1)/q_1)})F_1(e^{j\omega}) \\ &= e^{-j2\theta_1}e^{-j\omega N_1}e^{j\pi(m_1+1)N_1/q_1} \\ &\quad \times P_{1R}(\omega-(2m_1+3)\pi/2q_1) \\ &\quad \times P_{1R}(\omega-(2m_1+1)\pi/2q_1). \end{aligned} \tag{20}$$

After downsampled by p_1, (20) becomes

$$\begin{aligned} &p_1 H_1\left(zW_{q_1}^{m_1+1}\right)F_1(z) \downarrow p_1 \\ &\quad \overset{z=e^{j\omega}}{\longrightarrow} p_1 H_1(e^{j(\omega-2\pi(m_1+1)/q_1)})F_1(e^{j\omega}) \downarrow p_1 \\ &\quad = \sum_{i_1=0}^{p_1-1} e^{-j2\theta_1}e^{-j(\omega-2\pi i_1)N_1/p_1}e^{j\pi(m_1+1)N_1/q_1} \\ &\qquad \times P_{1R}((\omega-2\pi i_1)/p_1-(2m_1+3)\pi/2q_1) \\ &\qquad \times P_{1R}((\omega-2\pi i_1)/p_1-(2m_1+1)\pi/2q_1). \end{aligned} \tag{21}$$

With the parameter i_1 satisfying

$$p_1(m_1+1)\pi/q_1 + 2\pi i_1 = p_0\pi/q_0 \tag{22}$$

we get its frequency response in $[-\pi, \pi)$ as expressed in (12).

REFERENCES

[1] G. M. Shi, X. M. Xie, X. Y. Chen, and W. Zhong, "Recent advances and new design method in nonuniform filter banks," in *Proc. 2006 IEEE Int. Conf. Commun., Circuits, Syst.*, vol. 1, pp. 211–215.

[2] P. Q. Hoang and P. P. Vaidyanathan, "Non-uniform multirate filter banks: Theory and design," in *Proc. 1989 Int. Symp. Circuits Syst.*, pp. 371–374.

[3] K. Nayebi, T. P. Barnwell, and M. J. T. Smith, "Nonuniform filter banks: A reconstruction and design theory," *IEEE Trans. Signal Process.*, vol. 41, no. 3, pp. 1114–1127, Mar. 1993.

[4] J. Kovacevic and M. Vetterli, "Perfect reconstruction filter banks with rational sampling factors," *IEEE Trans. Signal Process.*, vol. 42, no. 6, pp. 2047–2066, Jun. 1993.

[5] B. Liu and L. T. Bruton, "The design of N-band nonuniform-band maximally decimated filter banks," in *Proc. 1993 Asilomar Conf. Circuits, Syst., Comput.*, pp. 1281–1285.

[6] T. Watanabe, Y. Shibahara, T. Kida, and N. Sugino, "Design of nonuniform FIR filter banks with rational sampling factors," in *Proc. 1998 IEEE Asia-Pacific Conf. Circuits Syst.*, pp. 69–72.

[7] R. V. Cox, "The design of uniformly and nonuniformly spaced pseudo quadrature mirror filters," *IEEE Trans. Acoust., Speech, Signal Process.*, vol. ASSP-34, no. 5, pp. 1090–1096, Oct. 1986.

[8] X. M. Xie, S. C. Chan, and T. I. Yuk, "Design of perfect-reconstruction nonuniform recombination filter banks with flexible rational sampling factors," *IEEE Trans. Circuits Syst. I*, vol. 52, no. 9, pp. 1965–1981, Sep. 2005.

[9] X. M. Xie, S. C. Chan, and T. I. Yuk, "Design of linear-phase recombination nonuniform filter banks," *IEEE Trans. Signal Process.*, vol. 54, no. 7, pp. 2809–2814, Jul. 2006.

[10] J. Princen, "The design of nonuniform modulated filter banks," *IEEE Trans. Signal Process.*, vol. 43, no. 11, pp. 2550–2560, Nov. 1995.

[11] B. J. Yoon and H. S. Malvar, "A practical approach for the design of nonuniform lapped transforms," *IEEE Signal Process. Lett.*, vol. 13, no. 8, pp. 469–472, Aug. 2006.

[12] J. J. Lee and B. G. Lee, "A design of nonuniform cosine modulated filter banks," *IEEE Trans. Circuits Syst. II*, vol. 42, no. 11, pp. 732–737, Nov. 1995.

[13] J. Li, T. Q. Nguyen, and S. Tantaratana, "A simple design method for near-perfect-reconstruction nonuniform filter banks," *IEEE Trans. Signal Process.*, vol. 45, no. 8, pp. 2105–2109, Aug. 1997.

[14] O. A. Niamut and R. Heusdens, "Subband merging in cosine-modulated filter banks," *IEEE Signal Process. Lett.*, vol. 10, no. 4, pp. 111–114, Apr. 2003.

[15] F. Argenti, B. Brogelli, and E. D. Re, "Design of pseudo-QMF banks with rational sampling factors using several prototype filters," *IEEE Trans. Signal Process.*, vol. 46, no. 6, pp. 1709–1715, Jun. 1998.

[16] S. Wada, "Design of nonuniform division multirate FIR filter banks," *IEEE Trans. Circuits Syst. II*, vol. 42, no. 2, pp. 115–121, Feb. 1995.

[17] T. Nagai, T. Futie, and M. Ikehara, "Direct design of nonuniform filter banks," in *Proc. 1997 IEEE Int. Conf. Acoust., Speech, Signal Process.*, vol. 3, pp. 2429–2432.

[18] X. Y. Chen, X. M. Xie, and G. M. Shi, "Direct design of near perfect reconstruction linear phase nonuniform filter banks with rational sampling factors," in *Proc. 2006 IEEE Int. Conf. Acoust., Speech, Signal Process.*, pp. III-253–III-256.

Radial Function Based Kernel Design for Time-Frequency Distributions

Sandun Kodituwakku, Rodney A. Kennedy, and Thushara D. Abhayapala

***Abstract*—A framework based on the n-dimensional Fourier transform of a radially symmetric function is introduced to design kernels for Cohen time-frequency distributions. Under this framework, we derive a kernel formula which generalizes and unifies Margenau–Hill, Born–Jordan, and Bessel distributions, using a realization based on a n-dimensional radial delta function. The higher order radial kernels suppress more cross-term energy compared with existing lower order kernels, which is illustrated by the time-frequency analysis of atrial fibrillation from surface electrocardiogram data.**

***Index Terms*—Bessel distribution, Born–Jordan distribution, Cohen class, kernel design, Margenau–Hill distribution, multidimensional Fourier transform, time-frequency distributions (TFDs).**

I. INTRODUCTION

Time-frequency distributions (TFDs) have been used extensively in analyzing nonstationary signals such as speech, radar, and physiological signals. They overcome the drawbacks of conventional Fourier analysis by simultaneously representing time and frequency for a given signal, thus enabling the analysis of the time variation of the spectrum content. A number of TFDs have been proposed in the past with their inherent advantages and drawbacks. The spectrogram, which is widely used as a TFD, has the inherent trade off between time and frequency resolutions. Later, the Wigner–Ville distribution was introduced with excellent time and frequency resolutions, but it suffers from cross-term

Manuscript received March 11, 2009; accepted January 30, 2010. Date of publication February 25, 2010; date of current version May 14, 2010. The associate editor coordinating the review of this manuscript and approving it for publication was Prof. Cedric Richard.

The authors are with the Applied Signal Processing Group, Research School of Information Sciences and Engineering, The Australian National University, Canberra, ACT 0200, Australia (e-mail: sandun.kodituwakku@anu.edu.au; thushara.abhayapala@anu.edu.au; rodney.kennedy@anu.edu.au).

Color versions of one or more of the figures in this correspondence are available online at http://ieeexplore.ieee.org.

Digital Object Identifier 10.1109/TSP.2010.2044252